CrystEngComm

ROYAL SOCIETY
OF CHEMISTRY

PAPER
Oksana Danylyuk *et al.*
Host–guest conformational adaptation in the crystal
complexes of pentamidine and *p*-sulfonato-calix[*n*]arenes

Check for updates

Host–guest conformational adaptation in the crystal complexes of pentamidine and *p*-sulfonato-calix[*n*]arenes

Kateryna Kravets, [iD] Mykola Kravets [iD] and Oksana Danylyuk [iD]*

The structural features of the host–guest crystal complexes of *p*-sulfonato-calix[*n*]arene series (**C4S**, **C6S** and **C8S**) with pentamidine are discussed. Smaller **C4S** and **C6S** provide their outer surface as a scaffold for exclusion complexation of pentamidine guests in the C-shaped conformation fitted to the curvature of the macrocycles, while their cavities contain solvent molecules. The largest **C8S** flattens into distorted pleated loop conformation with pentamidine guests taking advantage of the whole macrocyclic surface. The central hole of the **C8S** distorted pleated loop is available to alcohol solvent molecules, which do not interfere with the complexation of pentamidine. The host–guest complexation is also evident in the methanolic solution *via* ^{1}H NMR experiments, with a more pronounced effect of the largest **C8S** macrocyclic host.

Introduction

p-Sulfonato-calix[*n*]arenes are popular macrocyclic compounds for (bio)molecular recognition and integration into various supramolecular systems.[1,2] Their great advantages are high water solubility, biocompatibility and availability in the range of sizes defining cavity volumes and conformational properties of the macrocyclic skeletons. The smallest family member *p*-sulfonato-calix[4]arene **C4S** with a bowl-shaped cavity is well-known to attract metal ions and organic cations in the proximity of the anionic sulfonate rim.[3–5] The π-rich aromatic cavity can contain guest molecules and ions, as well as water molecule(s).[6,7] The typical cone conformation of **C4S** is sustained by a cyclic hydrogen bonding array between hydroxylic groups at the lower rim, as showcased in more than 300 crystal structures in the Cambridge Structural Database incorporating **C4S** locked in the cone conformation. The interesting exception is the sole example of the 1,3-alternate conformation of **C4S** in its complex with 4,4′-bipyridine crystallized at low pH.[8] The larger and more flexible *p*-sulfonato-calix[5]arene,[9–11] *p*-sulfonato-calix[6]arene,[12,13] *p*-sulfonato-calix[7]arene[14] and *p*-sulfonato-calix[8]arene[15,16] are able to adopt a range of conformations spanning from pleated loop to double-cavity up–up or up–down molecular shapes. The flattened pleated loop conformation of an extended molecular surface is particularly important for the controlled assembly and crystallization of proteins. For instance, *p*-sulfonato-calix[8]arene **C8S** can mask

Institute of Physical Chemistry Polish Academy of Sciences, Poland.
E-mail: odanylyuk@ichf.edu.pl

different patches of cationic protein cytochrome c giving rise to three crystal forms with different symmetries and interaction patterns.[17,18] Not only cavity inclusion is important, but also surface *exo* complexation can dictate the assembly to the limiting scenario when all protein–protein contacts in the crystal are eliminated due to large protein-calix[8]arene interfaces.[19] The nonrestricted conformational flexibility of **C8S** is also suitable for displaying a mutual induced fit molecular recognition with flexible partner molecules and construction of adaptive host–guest systems.[20]

Much progress has been achieved in the understanding of the complexation behavior of *p*-sulfonato-calix[*n*]arenes with small guest molecules, ions and even proteins.[21–23] However, despite several decades of intense research, many aspects of the assembly properties and predictability of their molecular architectures are still limited (especially for larger homologues of *n* > 4). Difficulties arise from their high conformational flexibility, oligo-ionic nature, formation of higher-order complexes, and competitive complexation of metal cations (counterions) and solvent molecules, among other factors. The structural studies on the **C6S** and **C8S** complexes are still scarce compared to the wealth of crystal structures available for **C4S**. It is accepted that the difference between **C4S** and larger homologues **C6S** and **C8S** is much more than a matter of size.[24] Therefore, we focus on the systematic investigation of the structural aspects of the series of macrocyclic hosts (**C4S**, **C6S** and **C8S**) with the same guest candidate, pentamidine, which is a World Health Organization Essential Medicine used as an antiprotozoal agent to treat the human sleeping sickness caused by *Trypanosoma brucei*. Previously, we showed that pentamidine adopts a compact U-shaped conformation upon inclusion into

the cavity of **C4S**.[25] Also, the supramolecular regime of **C4S**–pentamidine host–guest complexation can be changed from inclusion to exclusion by changing the complexation and crystallization media from water to water–alcohol mixtures. Here, we extend our studies to other solvent systems and larger macrocycles **C6S** and **C8S** (Fig. 1). We show that pentamidine is a suitable guest molecule for all three calixarene macrocyclic hosts; however, the host–guest interaction mode depends on the size of the macrocycle, as well as the solvent used for the crystallization. In all mixed solvent systems, **C4S** provides its outer surface as a scaffold for pentamidine molding without cavity penetration. The largest **C8S** adopts a distorted pleated loop shape with a "pseudo-calix[2]" shallow cavity to hold both folded and elongated conformations of pentamidine. We discuss different scenarios of host–guest conformational adaptation in the crystal complexes, and show how solvent molecules are actively engaged in these supramolecular assemblies.

Results and discussion

The outcome of the crystallisation of **C4S** with pentamidine isethionate depends on the solvent system used to solubilise host and guest components. Our previous study showed that **C4S**–pentamidine cocrystallisation in water suffers from the rapid microprecipitation due to the effective host–guest charge

neutralisation in the resulting inclusion complex (Fig. 2A).[25] The addition of other solvents to water improves the solubility, but at the same time alters the interaction in the supramolecular system and the structure of the final assembly. In contrast to the inclusion type complexation in aqueous media, the ^{1}H NMR spectrum in methanolic solution showed negligible shifts of pentamidine proton signals in the presence of **C4S**.[25] Following this line of study, we have attempted **C4S**–pentamidine crystallisation experiments in the mixed solvents, being successful (despite problems with microprecipitation) with water–isopropanol and water–acetone solvent mixtures. The crystallisation of **C4S** and pentamidine isethionate from water–isopropanol leads to the formation of crystalline complex **I** featuring exclusion binding of pentamidine guests to the macrocycle (Fig. 2B and C). The crystal structure was solved and refined in the monoclinic space group $P2_1/c$. The ASU consists of three crystallographically distinct **C4S** macrocycles, six pentamidines, six isopropanol and eleven water molecules. All macrocyclic cavities contain isopropanol guests hydrogen bonded to the sulfonate oxygen atoms at the upper rim (Fig. 2D and E). The inclusion of isopropanol molecules is also stabilised by C–H⋯π interactions between isopropanol methyl groups and aromatic subunits of **C4S**, and the shortest distance between $C_{(methyl)}$ and the centroid of the aromatic ring is 3.25 Å. The bowl cavity is additionally lidded by water molecule
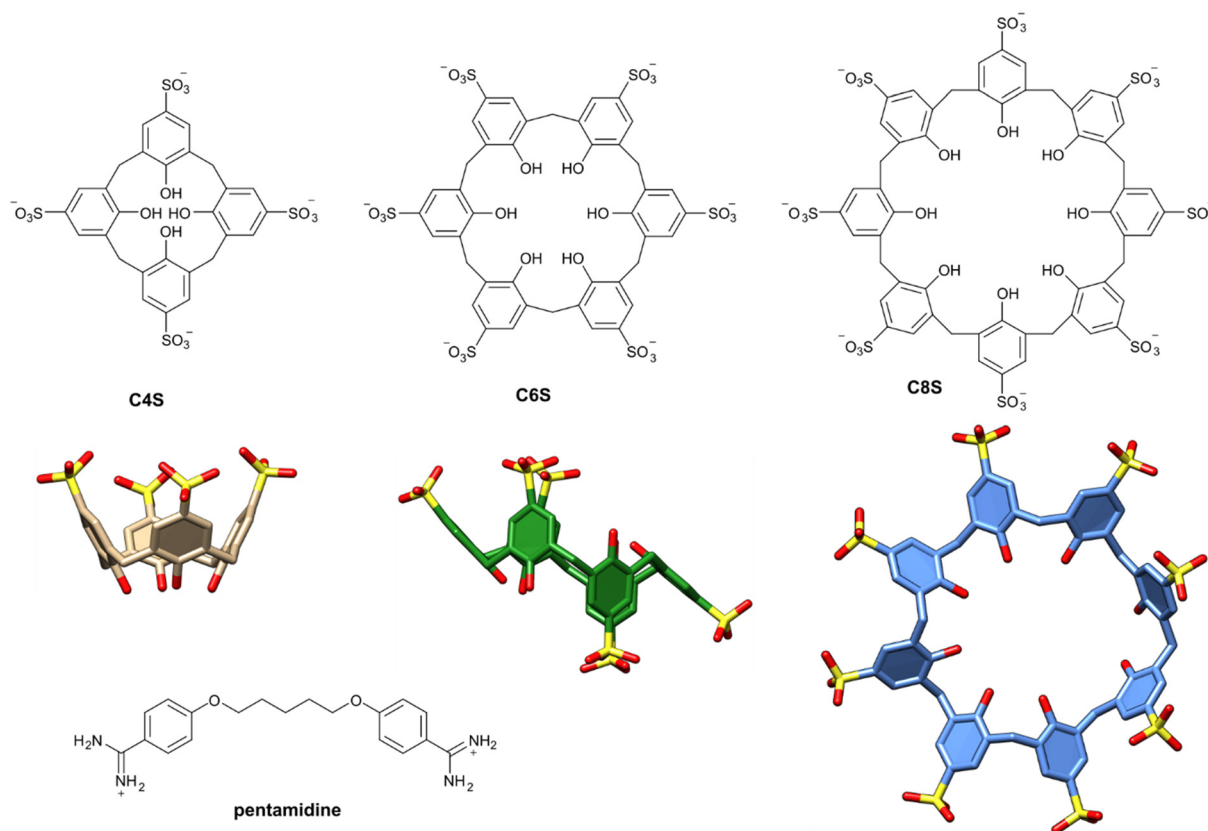

Fig. 1 Molecular structures of *p*-sulfonato-calix[4]arene (**C4S**) in cone conformation, *p*-sulfonato-calix[6]arene (**C6S**) in the inverted double partial cone conformation, *p*-sulfonato-calix[8]arene (**C8S**) in the deformed pleated loop conformation, and pentamidine used as a guest. The drawings of the conformations for **C4S**, **C6S** and **C8S** were generated using crystal structures described in this work.
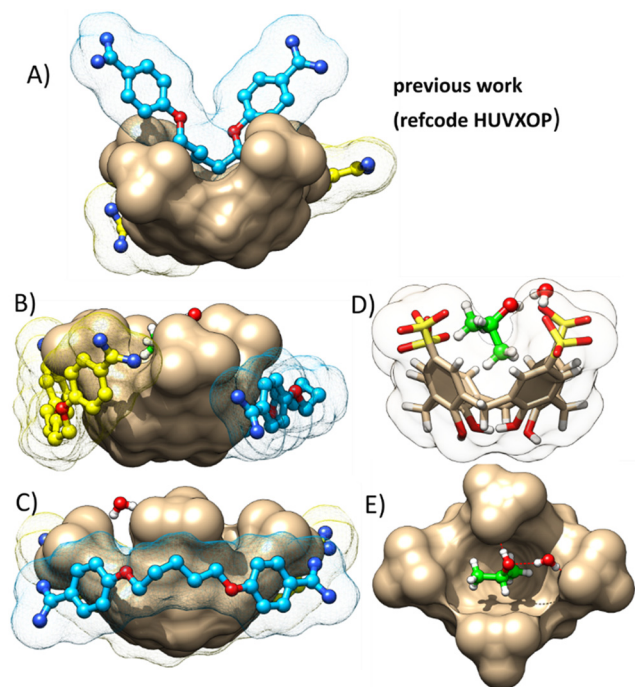
Fig. 2 Host–guest complexes of **C4S** with pentamidine crystallised from (A) water, previous work; one pentamidine molecule (in blue) is included in the cavity; another (in yellow) is complexed outside; (B and C) water–isopropanol mixture, this work; two pentamidine molecules mould to the external surface of the macrocycle; (D and E) the cavity is occupied by isopropanol molecule (in green) hydrogen bonded to the **C4S** upper rim. Water molecules and some hydrogen atoms omitted for clarity.

Fig. 3 (A) The amidinium–sulfonate hydrogen bonding between externally complexed pentamidine molecules and **C4S** in the complex **I** (crystallised from the water–isopropanol mixture); (B) part of the supramolecular assembly showing hydroxyl–sulfonate hydrogen bonds between adjacent **C4S** molecules in the crystal.

hydrogen bonded to the oxygen atom of the included isopropanol molecule and sulfonate oxygen of **C4S**.

The pentamidine guests residing outside the cavities are engaged in the amidinium–sulfonate hydrogen bonding with the anionic rim of **C4S** (Fig. 3A). The pentamidine molecules adopt a C-shaped conformation fitted to the external surface of the pinched cone geometry of calix[4]arene. The distances between O···O atoms directly bound to the central aliphatic chain of pentamidine molecules are in the range of 6.0–6.5 Å. The curvature is less pronounced relative to the pentamidine folded conformation (O···O distance of 4.4 Å) fixed by its inclusion into the **C4S** cavity, as shown in Fig. 1A. For comparison, pentamidine can adopt an extended rod-shaped conformation (O···O distance of 7.3 Å) in its inclusion complex with carboxylated pillar[5]arene of the rigid prismatic cavity accessible through two identical rims.[26]

In the studied complex, the competitive inclusion of the isopropanol molecule and exclusion-type binding of pentamidine are preferable over its strong compression to fit the inner space of the bowl-shaped calix[4]arene cavity. The presence of isopropanol cosolvent as an alternative guest for the cavity inclusion creates favorable conditions for the satiation of the hydrophobic effect and formation of the hydrogen bond between the included solvent molecule and macrocyclic host. In such a scenario, the amidinium–sulfonate hydrogen bonding synthons between *exo* complexed pentamidine and the anionic
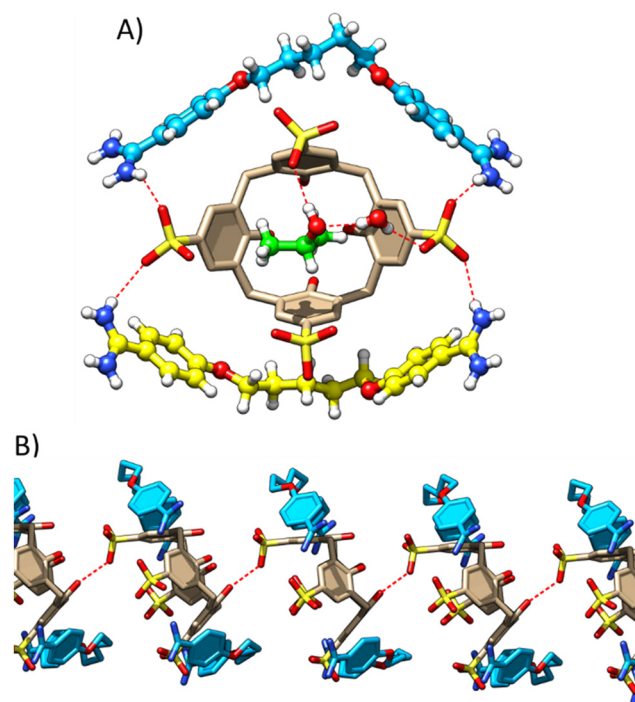
rim of **C4S** are excellently fulfilled due to the snug fit between the external surface of calix[4]arene and curved shape of pentamidine molecules (Fig. 3A). Most of the **C4S** external molecular surface is engaged in C–H···π and π···π interactions with either pentanediol chains or benzamidine moieties of adjacent pentamidines. Almost all calix[4]arene–calix[4]arene contacts are diminished, except O–H···O hydrogen bonding between the hydroxyl group at the lower rim and the sulfonate oxygen atom of the adjacent macrocycle (Fig. 3B). Due to the prevalence of **C4S**–pentamidine contacts engaging the external surface of the macrocycles, the classical bilayer organization is perturbed in the crystal structure. Instead, the supramolecular assembly consists of **C4S** individual columns separated by pentamidine bundles (Fig. 4). The main non-covalent interactions responsible for the supramolecular architecture are C–H···π contacts between **C4S** methylene groups (as donors) and benzamidine moieties of pentamidines (as acceptors), C–H···π interactions from pentamidine pentanediol chains towards **C4S** aromatic rings, as well as some π···π short contacts between the **C4S** external surface and benzamidine moieties of pentamidine.

The cocrystallisation of **C4S** and pentamidine isethionate from the water–acetone solvent mixture results in the formation of different crystal complex **II** (Fig. 5A and B). The crystal structure was solved and refined in the *I*2/*a* monoclinic space group. The ASU contains half of the **C4S** molecule residing on the 2-fold rotation axis, one pentamidine (disordered over two positions) complexed outside of the cavity, two acetone molecules and three water molecules.
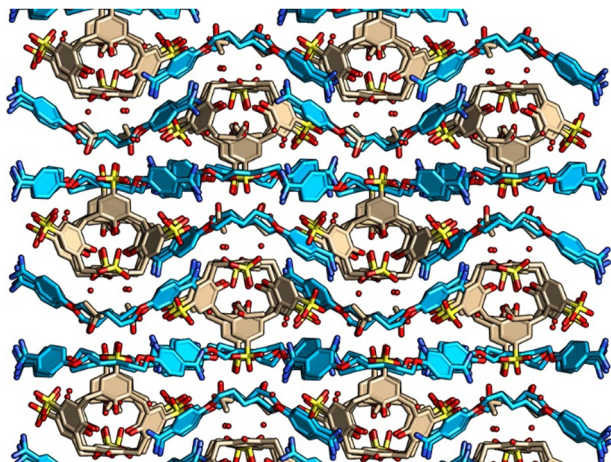
Fig. 4 Crystal packing in complex **I** (crystallised from the water–isopropanol mixture) viewed along the *b* direction; hydrogen atoms omitted for clarity; all pentamidine molecules shown in blue.

One of the acetone molecules (disordered by symmetry) fills the calix[4]arene cavity, while another resides close to the lower rim of the macrocycle (Fig. 5C and D). The exclusion complexation of pentamidine and preferential inclusion of solvent molecules are similar to the corresponding complex **I** obtained from water–isopropanol crystallization solvent. However, the mode of pentamidine molding to the **C4S** external surface and amidinium–sulfonate hydrogen bonding network is different than that to complex **I**.
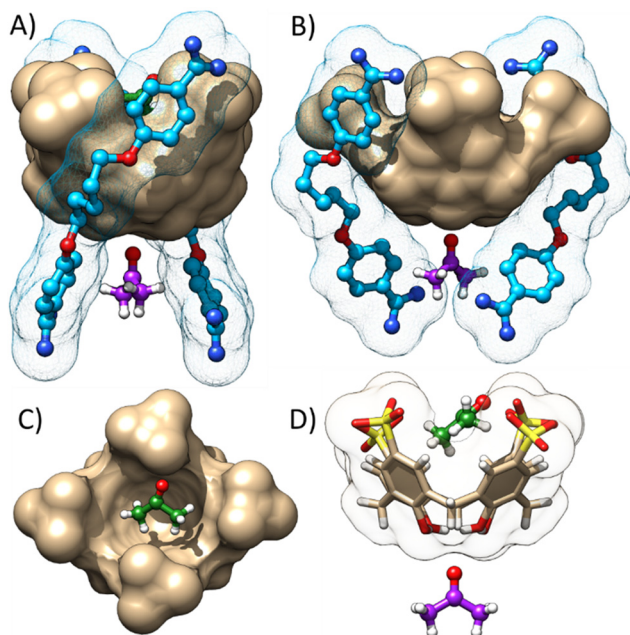
The presence of an additional acetone molecule at the hydrogen bonding distances to the lower rim of **C4S** is likely responsible for the change in the relative position of pentamidine guests. Due to the interaction of four lower rim hydroxyl groups with the acetone molecule, the hydroxyl–sulfonate hydrogen bonding between adjacent **C4S** molecules (present in the isopropanol complex **I**) is eliminated (Fig. 6A). The pentamidine molecules interact with the sulfonate upper rim *via* one benzamidinium moiety, while another benzamidinium group is headed in the direction of the lower rim to reach the sulfonate group of the neighboring **C4S** macrocycle (Fig. 6B). The conformation of the pentamidine guest is still C-shaped with O···O distances of 5.7 and 6.4 Å for the major and minor components of disorder, respectively. Adjacent **C4S** molecules in such a supramolecular assembly are far from each other being separated by acetone and pentamidine molecules.

The external surface of **C4S** is largely exposed to C–H···π contacts with pentamidine pentandiol chains, while calix[4]arene–calix[4]arene π···π interactions typical for **C4S** alternative (up–down) organization are absent. As can be expected, the crystal packing deviates from the well-known bilayer structural motif. Instead, the solid state assembly can be described as separated **C4S** columns connected by acetone and pentamidine molecules (Fig. 7). The overall assembly is sustained by C–H···π interactions from pentamidine pentandiol chains to **C4S** aromatic rings, while pentamidine aromatic groups are engaged in π···π interactions with aromatic groups of adjacent pentamidine molecules in the crystal structure.
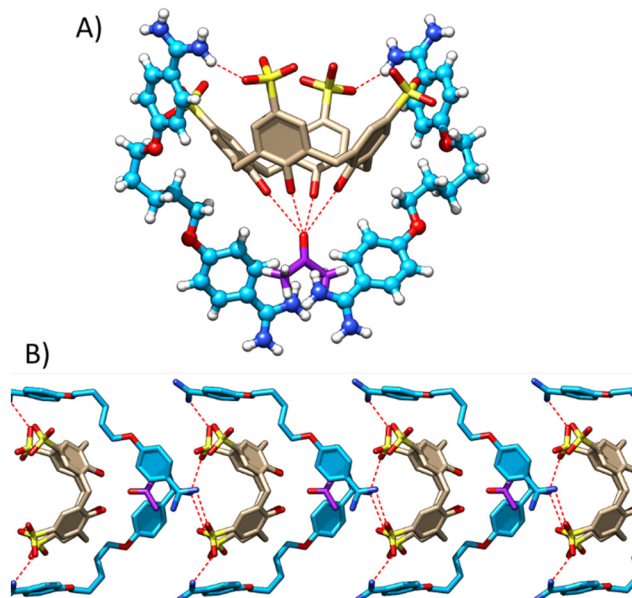

Fig. 5 Host–guest complex **II** of **C4S** with pentamidine crystallised from the water–acetone mixture. Water molecules and disorder omitted for clarity. (A and B) Two pentamidine molecules (in blue) mould to the external surface of the macrocycle; (C and D) the cavity is occupied by an acetone molecule (in green), and another acetone molecule (in violet) resides near the lower rim of the macrocycle.

Fig. 6 (A) The amidinium–sulfonate hydrogen bonding between externally complexed pentamidine molecules and **C4S**, and the acetone molecule near the **C4S** lower rim is at the hydrogen bonded distances with hydroxyl groups; (B) part of the supramolecular assembly showing amidinium–sulfonate hydrogen bonds between pentamidines and adjacent **C4S** molecules in the crystal complex **II**.
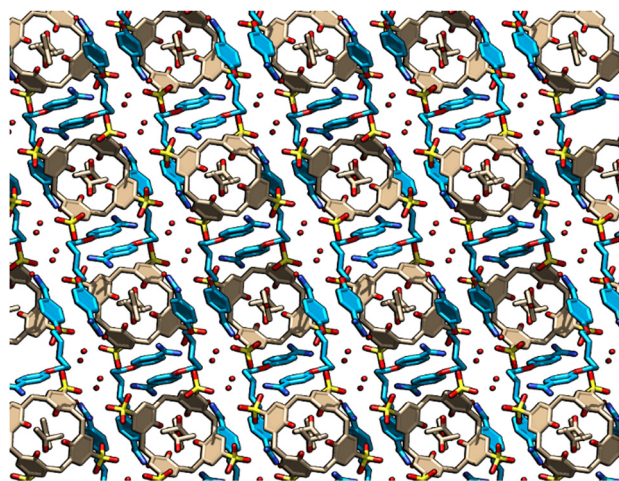
Fig. 7 Crystal packing in complex **II** (crystallised from the water–acetone mixture) viewed along the *b* direction; hydrogen atoms and disorder omitted for clarity; all pentamidine molecules shown in blue.

We have been successful in obtaining **C6S**–pentamidine single crystals of sufficient diffraction quality in the case of the water–methanol solvent mixture. The crystal structure of **C6S**–pentamidine complex **III** was solved and refined in the triclinic *P*1̄ space group. The ASU consists of one **C6S** as a hexa-anion, three pentamidine dications, two methanol molecules and eight water molecules (Fig. 8A and B). **C6S** adopts a 1,2,3-alternate conformation of compact shape featuring a small inner cavity filled with methanol molecules (Fig. 8C and D). The pentamidine molecules all of similar C-shaped curvature stick to the outer surface of the macrocycle. The inner space of the calix[6]arene molecule is geometrically not available for the interaction
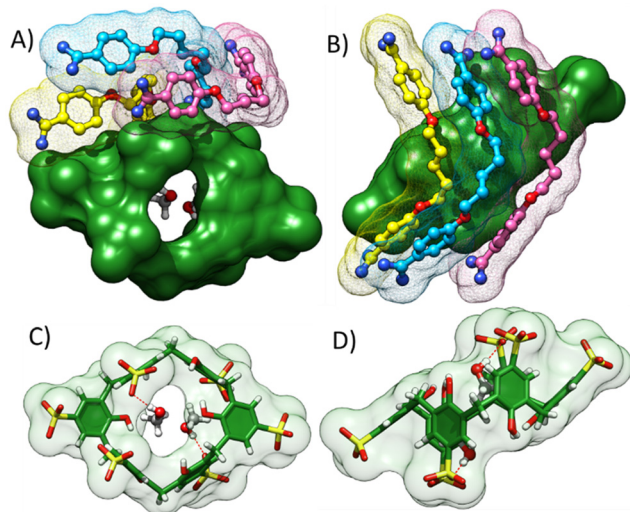

Fig. 8 Host–guest complex **III** of **C6S** with pentamidine crystallised from the water–methanol mixture. Water molecules and disorder omitted for clarity. (A and B) Three pentamidine molecules mould to the external surface of the macrocycle; (C and D) the cavity is occupied by two methanol molecules hydrogen bonded to sulfonate groups of the macrocycle.

with pentamidines. 1,2,3-Alternate conformation (also known as up–down or inverted double partial cone) is quite common for **C6S** host–guest complexes and assemblies,[27,28] even in the presence of metal cations coordinated to the upper rim of the macrocycle.[12,29] A CSD search (version 6.00) gives 51 hits on **C6S** structures, of which 15 are isostructural **C6S** assemblies with cucurbit[8]uril in the presence of various metal ions, with **C6S** in the flattened pleated loop conformation.[30] Of the remaining 36 crystal structures, 28 have **C6S** in some variants of the 1,2,3-alternate (up–down partial cone) conformation and 8 in the up–up double cone shape. In the majority of previously described crystal structures, **C6S** has two pseudo "calix[3]arene" cavities open in either opposite directions (up–down) or in the same direction (up–up). These partial cone cavities, albeit shallow, can accommodate various guests, as for instance crown ethers,[31] phenanthrolines,[32] amino acid L-leucine,[33] and others.[34]

A closer look at the **C6S** conformation in complex **III** reveals that both partial cones are collapsed due to inward tilting of two out of three walls framing "calix[3]arenes". Such distortion results in the complete disruption of intramolecular hydrogen bonding between OH phenolic groups usually observed in **C6S** structures. In the **C6S**–pentamidine complex, five hydroxyl groups of the macrocycle form hydrogen bonds with water molecules and one hydroxyl group interacts with sulfonate oxygen atoms of adjacent **C6S** molecules. Only a small entrance to the inner space of the macrocycle remains available to let in the methanol molecules.

The proximity of two anionic sulfonate groups in the distorted up–down **C6S** conformation is compensated with their involvement in the charge-assisted hydrogen bonding with cationic amidinium donors of pentamidine molecules (Fig. 9A). Each of the six sulfonate groups is engaged in this hydrogen bonding, interacting with one or more amidinium groups. All three pentamidine molecules are in the C-shaped conformation fitting to the shape of each other and the external surface of the macrocycle. The distances between O⋯O atoms directly bound to the central aliphatic chain are in the range of 5.9–6.0 Å. The pentamidine conformation is again intermediate between the fully extended shape observed in the case of the host–guest complex with pillar[5]arene (O⋯O distance of 7.3 Å)[26] and the folded one (O⋯O distance of 4.4 Å) induced by pentamidine inclusion into the **C4S** cavity.[25] The pentandiol linkers are at the C–H⋯π contact distances with external aromatic walls of calix[6]arene, while benzamidine aromatic moieties interact with each other *via* π⋯π stacking in the offset geometry (Fig. 9C). The host–guest interactions occur mainly at the anionic rim of the macrocycle as salt bridges and at the external surface of calix[6]arene, with its internal surface unavailable for pentamidine molecules. Two external aromatic walls of the macrocyclic molecule participate in calix[6]arene–calix[6]arene interactions as hydroxyl–sulfonate hydrogen bonds of 2.75 Å (Fig. 9B), together with C-H⋯π and π⋯π contacts. The combination of these interactions assembles **C6S** molecules into individual rows running along the *a* direction. The solid
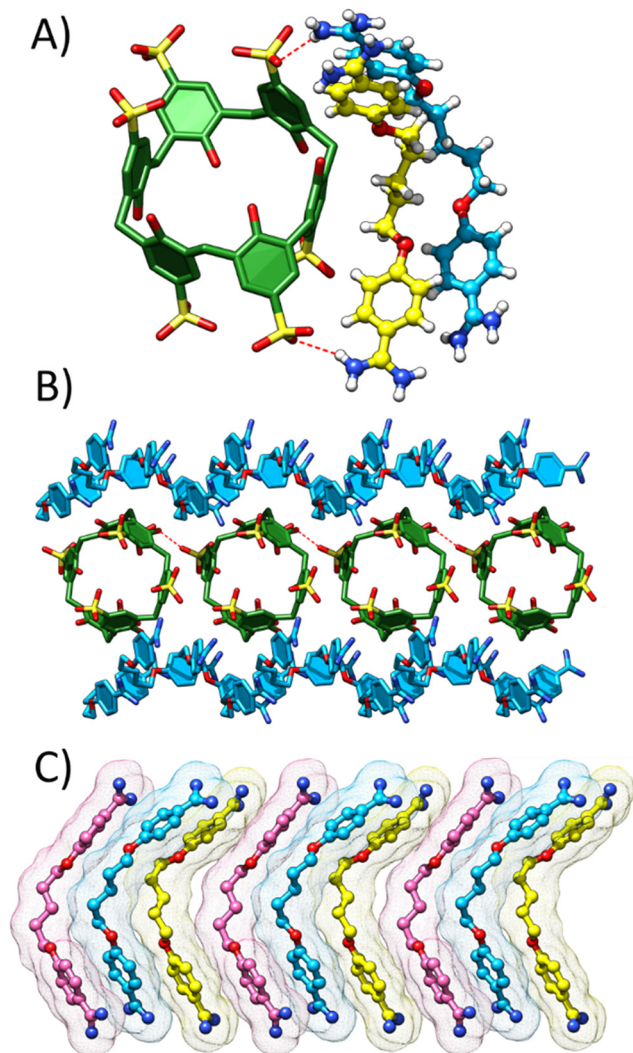
Fig. 9 (A) The amidinium–sulfonate hydrogen bonding between externally complexed pentamidine molecules and **C6S** in complex **III**; (B) part of the supramolecular assembly showing hydroxyl–sulfonate hydrogen bonds between adjacent **C6S** molecules; (C) C-shaped pentamidine molecules are in close contact with each other due to π⋯π stacking in the offset geometry between benzamidinium moieties.

Fig. 10 Crystal packing of **C6S**–pentamidine complex **III** (crystallized from the water–methanol mixture) viewed along the *a* direction; hydrogen atoms and disorder omitted for clarity; all pentamidine molecules shown in blue.

presence of **C6S**. The more pronounced upfield shifts are observed for the aromatic protons of benzamidinium groups (a and b). The upfield shifts of all proton resonances of pentamidine suggest the inclusion host–guest complexation in the methanolic solution in contrast to the exclusion type complexes in the determined crystal structures. We previously established the inclusion possibility of the simple benzamidine ligand into the **C4S** cavity both in the aqueous solution and several host–guest crystal complexes.[35]

The **C8S**–pentamidine cocrystallisation trials yielded single crystals in the water–ethanol and water–isopropanol solvent mixtures. Unexpectedly, the problem of microprecipitation encountered for **C4S** and **C6S** crystallisation experiments has not disturbed the crystal growth in the case of **C8S** complexes.

state architecture is built from separate rows of **C6S** and pentamidine molecules sewn together *via* C–H⋯π interactions between pentanediol linkers of pentamidines and aromatic rings of calix[4]arenes (Fig. 10). The cationic amidinium groups are clustering near sulfonate groups in the hydrophilic region of the structure. The rows of **C6S** are separated by hydrophobic bundles of pentamidine aliphatic linkers.

We have also looked at the host–guest complexation of pentamidine with **C6S** in CD₃OD solution using ¹H NMR spectroscopy (Fig. 11). The addition of pentamidine isethionate to **C6S** methanolic solution resulted in the rapid formation of a suspension/precipitate, which partially dissolved upon gentle heating. The ¹H NMR spectra showed small shifts in the aliphatic proton signals of pentamidine (f and g) in the
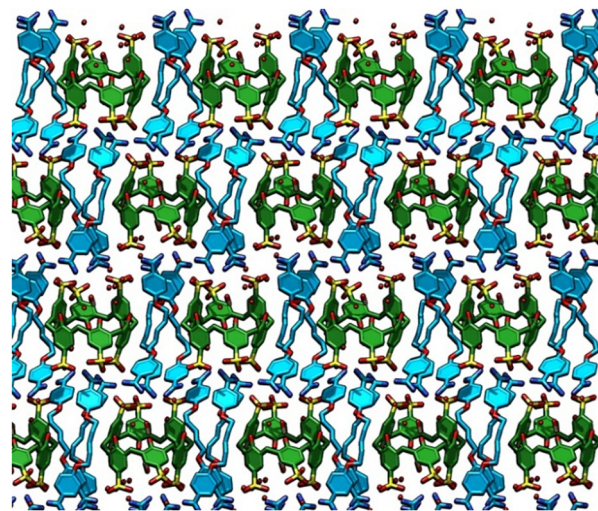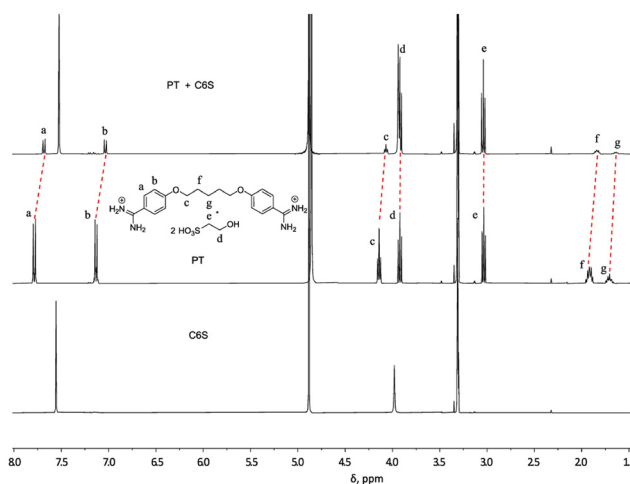

Fig. 11 ¹H NMR spectra of **C6S**, pentamidine isethionate (**PT**) and host–guest complex – in the presence of some precipitate, recorded on an Agilent 400 MHz instrument at room temperature in CD₃OD. c(**C6S**) = 4 mM, c(pentamidine) = 4 mM.
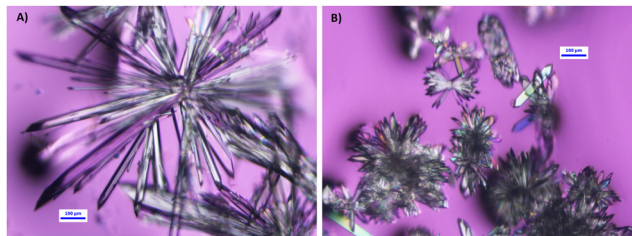
Fig. 12 Photo micrographs of **C8S**–pentamidine crystal complexes obtained from water–ethanol (A) and water–isopropanol (B) solvent mixtures. Micrographs taken under polarized light.

As a result, nicely shaped prismatic crystals have been observed under a microscope the next day after crystallisation set-ups (Fig. 12). Two crystal structures of complexes **IV** (obtained from water–ethanol) and **V** (from the water–isopropanol mixture) appeared to be isostructural. The crystal of complex **IV** gave a diffraction dataset of better quality, and this crystal structure is discussed as exemplary. The crystal structure of **C8S**–pentamidine complex **IV** was solved and refined in the monoclinic space group $C2/c$. There are two crystallographically unique **C8S** molecules of similar conformations in the asymmetric unit, besides eight pentamidines, ethanol and water molecules (disordered). Complex **IV** is highly solvated with 36.7 water molecules introduced in the structure model (38.2 water molecules for complex **V**). The implementation of the SQUEEZE/PLATON (ref. 36) procedure on the solvent-free models to account for disordered solvent molecules as a diffuse contribution to the overall scattering resulted in improved *R*-values and bond precision. The final refinement results for the atomistic model for the disordered solvent and alternative SQUEEZE treatment are summarized in the Experimental section, and both versions of CIF files are deposited in the CSD.

Both calix[8]arenes adopt a flattened conformation similar to the pleated loop but with two adjacent subunits in the up–up orientation forming a pseudo-calix[2] shallow cavity (Fig. 13). Each **C8S** binds four pentamidine guests, two molecules on one side of the surface and two on the opposite side. While in the perfect pleated loop conformation, both sides of the macrocycle are identical; here, the distortion results in the de-symmetrization and distinction of two surfaces – one with the pseudo-calix[2] cavity and two grooves, and another with three grooves (Fig. 13A–C). The central hole of the macrocycle is occupied by an alcohol solvent molecule (ethanol in complex **IV** and isopropanol in complex **V**) hydrogen bonded to one of the phenolic groups stabilizing the **C8S** conformation (Fig. 13D and E).

In the true pleated loop conformation, eight hydroxyl groups are arranged in the almost planar hydrogen bonded cyclic array as shown in Fig. 14A.[37] The plane defined by eight coplanar oxygen atoms showcases four identical grooves (on either side of the macrocycle) generated by the kinking of the methylene bridging groups alternatively above and below this virtual plane (Fig. 14C). In the discussed host–guest complex **IV**, the intramolecular hydrogen bonded array is disrupted (Fig. 14B). In this **C8S** conformation, six aryl rings
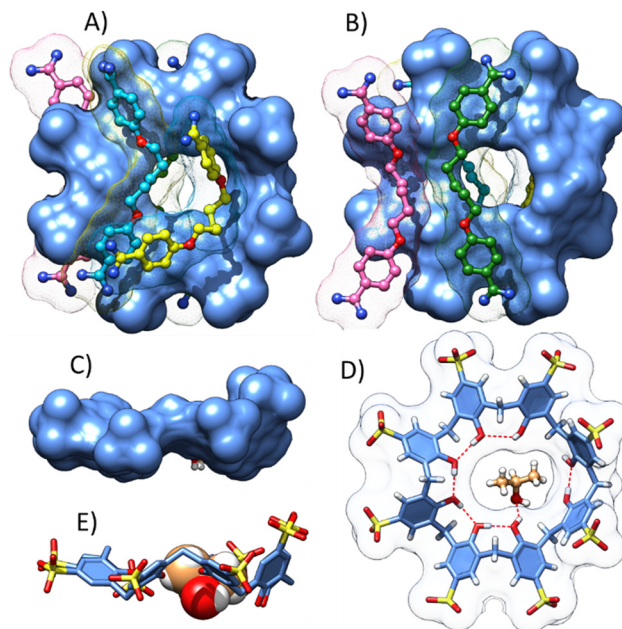

Fig. 13 (A–C) Host–guest complex **IV** of **C8S** with pentamidine crystallised from the water–ethanol mixture. The calix[8]arene molecule adopts a distorted pleated loop conformation with a pseudo-calix[2] shallow cavity occupied by pentamidine in the most bent conformation (coloured in yellow); three other pentamidine molecules (coloured in blue, rose and green) fit to the grooves and bumps on the **C8S** surface. The central hole of the macrocycle holds one ethanol molecule (not shown for clarity). (D and E) The central hole in the isostructural complex **V** is occupied by isopropanol molecule hydrogen bonded to one of the hydroxyl groups of calix[8] arene. Water molecules and disorder omitted for clarity.

follow a continuous "pleated ribbon" shape sustained by five intramolecular hydrogen bonds. The deformation can be described as the upright placement of two contiguous aryl moieties (pseudo-calix[2]) relative to the plane defined by six oxygen atoms of the "pleated loop" part of the molecule (Fig. 14D). The methylene carbon atom bridging these two aryl rings is coplanar with six oxygen atoms, while two hydrogen bonded hydroxyl groups within pseudo-calix[2] deformation are projected below this virtual plane. For comparison, none of the 23 crystal structures of different **C8S** assemblies deposited in the Cambridge Structural Database shows the same distorted pleated loop shape. In the previously reported host–guest, coordination and metallo-supramolecular structures of **C8S**, the macrocycle shows a wide span of conformations between extreme inverted double cone (also known as up–down double cone) and flattened pleated loop shapes.[38–41] The **C8S** molecule can adopt an unusual conformation as a combination of the pseudo "calix[3]arene" cavity and pleated loop in the presence of tetraphenylphosphonium and aquated ytterbium(III) ions.[42] The unrestricted conformational flexibility of the macrocyclic skeleton has been well recognized also in *p-tert*-butyl-calix[8] arene coordination complexes[43] and solvate structures.[44]

All pentamidines exhibit various degrees of bending adjusting to the bumps, hollows and their combination at
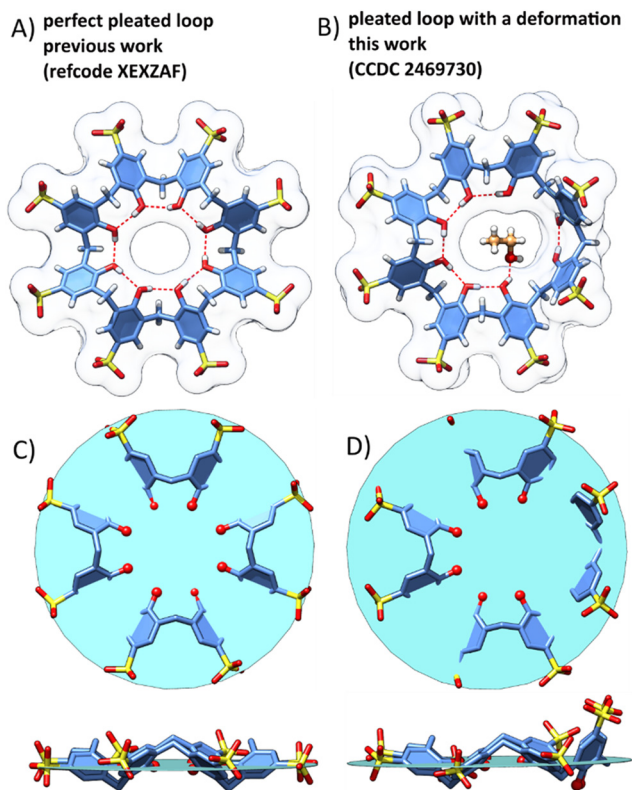
Fig. 14 (A) The perfect pleated loop conformation of **C8S** of circular hydrogen bonding array at the lower rim, previous work (refcode XEXZAF). (B) The deformed pleated loop conformation of **C8S** in its host–guest complex **V** with pentamidine; circularity of hydrogen bonding is disrupted, this work. (C) In the true pleated loop molecular shape, all eight hydroxyl oxygen atoms are coplanar; the virtual plane defined by eight oxygen atoms shown in blue colour. (D) In the deformed pleated loop conformation, only six out of eight oxygen atoms are coplanar, and the remaining two hydroxyl groups are positioned below the plane due to the upright orientation of two juxtaposed aryl rings.

which guests reside. The most defined curvature on the **C8S** surface is of "pseudo-calix[2]" shape capable of distinct U-shape guest folding (pentamidine molecule coloured in yellow in Fig. 13A). A similar conformational fixing of the pentamidine molecule is observed upon its inclusion into the **C4S** cavity, as shown in Fig. 2A. Neither of the pentamidine molecules is in the fully elongated conformation, as in three crystal forms of the host–guest inclusion complex with carboxylated pillar[5]arene.[26] The inclusion of pentamidine into larger pillar[6]arene also does not hamper its elongated shape as the macrocycle is able to squeeze around the rod-like guest to maximize the host–guest interactions.[45] Two reported and deposited structures of pentamidine isethionate salts in the CSD comprise pentamidine in the elongated shape.[46,47] In all these structures, the torsional angles of the extended penta-nediol linker are close to 180.0° typical for the energetically preferred *anti* conformation. The central chain torsion angles of all pentamidine molecules in the **C8S** host–guest ensemble are distorted, and the exemplary angles are −78°, 72° and 83°. The crumpled conformation of the central linkers causes

overall shortening of pentamidine molecules and better fitting to the curved surface of the macrocycle, enabling C–H⋯π, cation⋯π, and hydrogen bonding possibilities with **C8S**. The most elongated pentamidine molecule interacts *via* amidinium–sulfonate hydrogen bonding with sulfonate groups on the opposite edges of the pleated loop part of the macrocycle (Fig. 15A). The most folded pentamidine shows C–H⋯π and C–H⋯O close contacts of its pentandiol chain in the "pseudo-calix[2]" spot of the **C8S** surface, while its benzamidinium moieties point away towards adjacent **C8S** molecules in the crystal structure. Overall, the **C8S**–penta-midine ensemble can be considered as a mutually induced fit structure as both highly flexible host and guest molecules adapt their geometry for the optimal complexation.

The majority of the **C8S** surface is engaged in the various contacts with guest molecules. The external surface of the "pseudo-calix[2]" bump is covered by adjacent pentamidine. The sole interaction between neighboring **C8S** molecules in the crystal is hydroxyl–sulfonate hydrogen bonding (O–H⋯O distances are 2.59 and 2.70 Å), as shown in Fig. 15B. Besides this hydrogen bonding, there is no possibility for the **C8S** oligomerization through surface wall interactions. All **C8S** molecules are well separated from each other by thick bundles of pentamidines shown in yellow color in Fig. 16. The supramolecular architecture is supported by multiple **C8S**–pentamidine interactions; these include π⋯π contacts in the face-to-face and edge-to-face orientations between **C8S** aromatic rings and pentamidine benzamidine groups, C–H⋯π interactions from macrocycle methylene groups towards pentamidine aromatic moieties, and C–H⋯π interactions from pentamidine pentanediol chains to
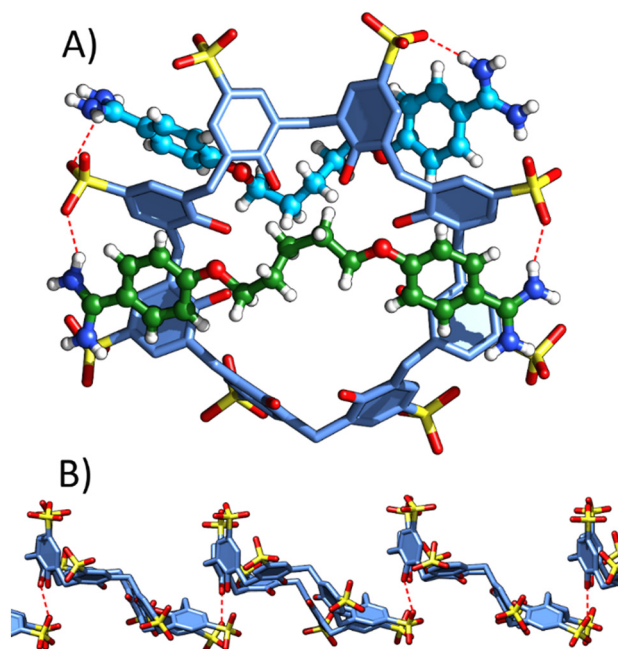

Fig. 15 (A) The amidinium–sulfonate hydrogen bonding between selected pentamidine molecules and sulfonate groups in the pleated loop part of calix[8]arene in complex **IV**; (B) intermolecular hydroxyl–sulfonate hydrogen bonding between adjacent **C8S** molecules.
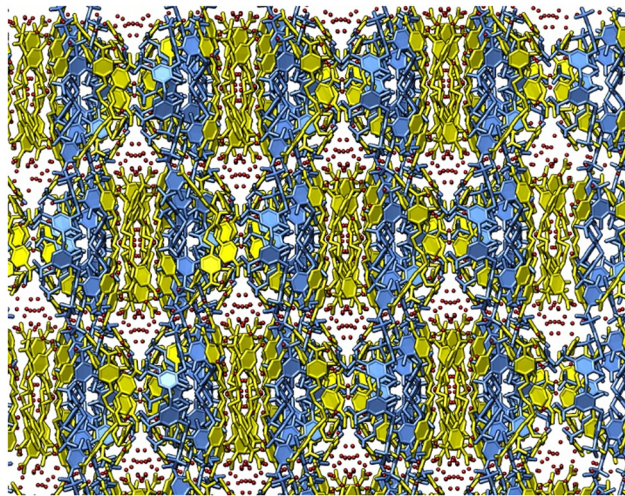
Fig. 16 Crystal packing of C8S–pentamidine complex IV; hydrogen atoms and disorder omitted for clarity; all pentamidine molecules shown in yellow colour, all C8S molecules are in cornflower blue colour.
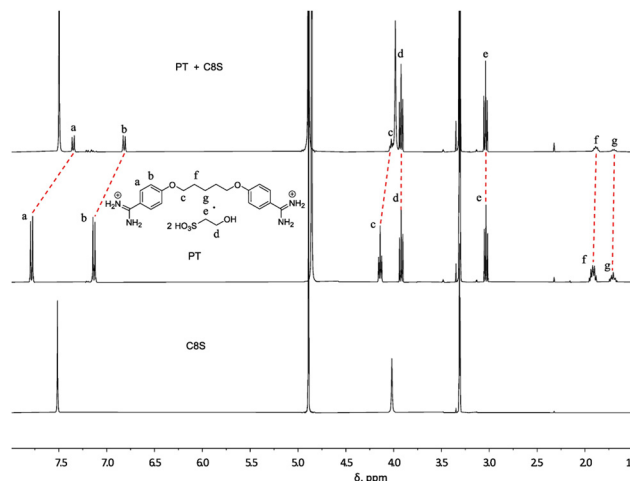

Fig. 17 ^{1}H NMR spectra of C8S, pentamidine isethionate (PT) and host–guest complex – in the presence of some precipitate, recorded on an Agilent 400 MHz instrument at room temperature in CD_3OD. c(C8S) = 4 mM, c(pentamidine) = 4 mM.

calix[8]arene aromatic rings. Additionally, $\pi\cdots\pi$ and C–H$\cdots\pi$ interactions between adjacent pentamidine molecules can be identified within their bundles. Multiple water molecules in the interconnected channels take approximately 20% of the crystal volume. In the previously reported C8S sodium salt structures, the stacking of adjacent macrocycles is efficiently realized through pleated loop surface interactions and coordination of metal cations.[37,48] Also, C8S can oligomerize into dimeric or trimeric macrocycle supramolecular synthons in the crystal structures with selected proteins.[49,50]

The host–guest complexation between pentamidine and C8S in CD_3OD solution was confirmed by ^{1}H NMR spectroscopy (Fig. 17). Upon mixing C8S and pentamidine solutions, some precipitate formed, which partially dissolved upon gentle heating. The ^{1}H NMR spectra showed minor shifts of the aliphatic proton signals of pentamidine (f and g) in the presence of C8S. Large upfield shifts are visible for the aromatic protons of benzamidinium groups (a and b), even more pronounced compared to the shifts observed in the case of the C6S–pentamidine complex. Such large shifts of aromatic proton resonances indicate deep inclusion of the guest benzamidinium groups into the host cavity. Thus, it might be expected that the C8S molecule adopts a more globular shape of the substantial cavity in the solution relative to the flattened pleated loop conformation observed in the crystal complex.

Conclusions

Host–guest crystal complexes between p-sulfonato-calix[n]arenes and pentamidine show a high degree of structural and supramolecular adaptation in terms of induced fit, mutual induced fit and competitive/cooperative inclusion of solvent molecules. The calix[n]arene–pentamidine interactions are efficiently realized not only in the classical inclusion mode requiring pentamidine folding into compact U-shape,[25] but also through exo-wall surface interactions involving pentamidine

C-shaped gentler bending. Pentamidine molecules in the C-shaped conformation mould closely to the outer surface curvature of C4S and C6S while forming amidinium–sulfonate hydrogen bonding by two terminal benzamidinium moieties. Indeed, pentamidine as a guest is able to significantly perturb the common bilayer arrangement of C4S and C6S molecules usually realized through a combination of $\pi\cdots\pi$ and C-H$\cdots\pi$ interactions between external walls of adjacent macrocycles. The association of pentamidine molecules around external surface of the macrocycles disrupts direct calixarene–calixarene contacts. This reminds the use of pentamidine in medicinal chemistry as a perturbant molecule, which disrupts the integrity of the bacteria outer membrane by disordering the quasi-crystalline structure of its LPS monolayer.[51]

The largest C8S molecule flattens into distorted pleated loop conformation with pentamidine guests taking advantage of the whole macrocyclic surface. In this conformation, the differentiation between the inner and outer surface is blurred, as the C8S shape evolved towards a solid torus like structure (with deformation) in comparison to the cone shape of the smallest homologue C4S. The central hole of the C8S distorted pleated loop is available to alcohol solvent molecules. Again, in this crystal complex, all calixarene–calixarene contacts are diminished (except scarce hydroxyl–sulfonate hydrogen bonding) due to rich C8S–pentamidine interactions. Potentially, the portfolio of the possible conformations for C8S can be further expanded, pursuing the cocrystallisation and structural characterisation of its complexes and assemblies. These can benefit the growing application of macrocycles as tectons in directing protein assembly and crystal engineering.[52]

Experimental

pentamidine isethionate, p-sulfonato-calix[4]arene, p-sulfonato-calix[6]arene and p-sulfonato-calix[8]arene were purchased from

TCI Europe and used as received. ^{1}H NMR spectra were recorded on an Agilent 400 MHz instrument using CD$_3$OD solvent at room temperature.

Crystallisation conditions

Complex I. 5 mg of **C4S** was dissolved in a 0.5 mL of 1:1 water–isopropanol mixture. The solution of 4.6 mg of pentamidine isethionate in the 0.5 mL of 1:1 water–isopropanol mixture was slowly added to the solution of **C4S**. The clouding of the solution was observed followed by some microprecipitation. Prismatic shaped crystals of complex **I** suitable for diffraction were found after several days.

Complex II. 5 mg of **C4S** was dissolved in a 0.5 mL of 1:1 water–acetone mixture. The solution of 4.6 mg of pentamidine isethionate in the 0.5 mL of 1:1 water–acetone mixture was slowly added to the solution of **C4S**. Rapid clouding of the solution was observed followed by microprecipitation. Plate-like crystals of complex **II** suitable for diffraction were found within the precipitate after several days.

Complex III. 20 mg of **C6S** was dissolved in a 0.5 mL of 1:1 water–methanol mixture. The solution of 18.3 mg of pentamidine isethionate in the 0.5 mL of 1:1 water–methanol mixture was slowly added to the solution of **C6S**. Rapid clouding of the solution was observed followed by microprecipitation. Prismatic crystals of complex **III** suitable for diffraction were found within the precipitate after 10 days.

Complex IV. 20 mg of **C8S** was dissolved in a 1 mL of 1:1 water–ethanol mixture. The solution of 9.1 mg of pentamidine isethionate in the 1 mL of 1:1 water–ethanol mixture was slowly added to the solution of **C8S**. The clouding of the solution was observed. Prismatic crystals of complex **IV** suitable for diffraction were found the next day.

Complex V. 20 mg of **C8S** was dissolved in a 1 mL of 1:1 water–isopropanol mixture. The solution of 9.1 mg of pentamidine isethionate in the 1 mL of 1:1 water–isopropanol mixture was slowly added to the solution of **C8S**. The clouding of the solution was observed. Prismatic crystals of complex **V** suitable for diffraction were found the next day.

Crystallography

The crystals were embedded in the inert perfluoropolyalkylether (viscosity: 1800 cSt; ABCR GmbH) and mounted using Hampton Research Cryoloops. The crystals were flash cooled to 100.0(1) K in a nitrogen gas stream and kept at this temperature during the experiments. The X-ray data were collected on a SuperNova Agilent diffractometer using CuKα radiation (λ = 1.54184 Å). The data were processed with CrysAlis PRO software. Structures were solved by direct methods and refined using SHELXL[53] under WinGX.[54] The crystal complexes **IV** and **V** are highly solvated with many disordered water molecules introduced in the structure models. Alternatively, to address the solvent disorder issue the SQUEEZE/PLATON method[36] was implemented on **IV** and **V**. The contribution of disordered water molecules removed by SQUEEZE has been included in the overall formula, formula weight, density, etc. The refinement

details for complexes **IV** and **V** with and without SQUEEZE are given below. The figures were prepared using Chimera.[55]

Crystal data for complex I. 3(C$_{28}$H$_{20}$O$_{16}$S$_4$)·6(C$_{19}$H$_{26}$N$_4$O$_2$)·6(C$_3$H$_8$O)·11(H$_2$O), M_r = 4835.4, colourless prisms, monoclinic, space group $P2_1/c$, a = 23.6106(1), b = 30.3731(2), c = 31.5092(2) Å, β = 91.424(1)°, V = 22589.1(2) Å^3, Z = 4, ρ_{calc} = 1.42 g cm^{-3}, μ(CuKα) = 1.89 mm^{-1}, θ_{max} = 70.1°, 145 447 reflections measured, 42 468 unique, 2977 parameters, R = 0.060, wR = 0.162 (R = 0.075, wR = 0.174 for all data). GooF = 1.03. CCDC 2469729.

Crystal data for complex II. (C$_{28}$H$_{20}$O$_{16}$S$_4$)·2(C$_{19}$H$_{26}$N$_4$O$_2$)·2(C$_3$H$_6$O)·6(H$_2$O), M_r = 1649.8, colourless plate, monoclinic, space group $I2/a$, a = 25.024(3), b =13.519(2), c = 24.370(4) Å, β = 108.954(17)°, V = 7798(2) Å^3, Z = 4, ρ_{calc} = 1.41 g cm^{-3}, μ(CuKα) = 1.86 mm^{-1}, θ_{max} = 65.1°, 44 737 reflections measured, 6650 unique, 803 parameters, R = 0.123, wR = 0.355 (R = 0.157, wR = 0.399 for all data). GooF = 1.12. CCDC 2469727.

Crystal data for complex III. (C$_{42}$H$_{30}$O$_{24}$S$_6$)·3(C$_{19}$H$_{26}$N$_4$O$_2$)·2(CH$_4$O)·8.3(H$_2$O), M_r = 2351.5, colourless prisms, triclinic, space group $P\bar{1}$, a = 12.3629(5), b = 16.5072(7), c = 28.5794(17) Å, α = 85.914(4), β = 85.670(4), γ = 74.715(4)°, V = 5602.0(5) Å^3, Z = 2, ρ_{calc} = 1.39 g cm^{-3}, μ(CuKα) = 1.90 mm^{-1}, θ_{max} = 60.9°, 31 818 reflections measured, 16 703 unique, 1774 parameters, R = 0.117, wR = 0.310 (R = 0.173, wR = 0.350 for all data). GooF = 1.06. CCDC 2469726.

Crystal data for complex IV. 2(C$_{56}$H$_{40}$O$_{32}$S$_8$)·8(C$_{19}$H$_{26}$N$_4$O$_2$)·2.5(C$_2$H$_6$O)·36.7(H$_2$O), M_r = 6478.8, colourless prisms, monoclinic, space group $C2/c$, a = 33.9061(5), b = 41.7359(5), c = 46.4819(7) Å, β = 94.332(2),° V = 65588.7(16) Å^3, Z = 8, ρ_{calc} = 1.31 g cm^{-3}, μ(CuKα) = 1.78 mm^{-1}, θ_{max} = 66.6°, 637 017 reflections measured, 57 878 unique, 4955 parameters, R = 0.127, wR = 0.325 (R = 0.191, wR = 0.394 for all data). GooF = 1.18. CCDC 2469730.

Crystal data for complex IV_squeeze. 2(C$_{56}$H$_{40}$O$_{32}$S$_8$)·8(C$_{19}$H$_{26}$N$_4$O$_2$)·2(C$_2$H$_6$O)·48.3(H$_2$O), M_r = 6664.3, colourless prisms, monoclinic, space group $C2/c$, a = 33.9061(5), b = 41.7359(5), c = 46.4819(7) Å, β = 94.332(2),° V = 65588.7(16) Å^3, Z = 8, ρ_{calc} = 1.35 g·cm^{-3}, μ(CuKα) = 1.82 mm^{-1}, θ_{max} = 66.6°, 637 017 reflections measured, 57 878 unique, 4340 parameters, R = 0.114, wR = 0.309 (R = 0.174, wR = 0.380 for all data). GooF = 1.14. CCDC 2482200.

Crystal data for complex V. 2(C$_{56}$H$_{40}$O$_{32}$S$_8$)·8(C$_{19}$H$_{26}$N$_4$O$_2$)·2(C$_3$H$_8$O)·38.2(H$_2$O), M_r = 6511.3, colourless prisms, monoclinic, space group $C2/c$, a = 34.1908(18), b = 41.4283(12), c = 46.9910(18) Å, β = 95.325(5),° V = 66 274(5) Å^3, Z = 8, ρ_{calc} = 1.31 g·cm^{-3}, μ(CuKα) = 1.76 mm^{-1}, θ_{max} = 58.9°, 129 320 reflections measured, 47 500 unique, 4456 parameters, R = 0.133, wR = 0.333 (R = 0.323, wR = 0.496 for all data). GooF = 0.93. CCDC 2469728.

Crystal data for complex V_squeeze. 2(C$_{56}$H$_{40}$O$_{32}$S$_8$)·8(C$_{19}$H$_{26}$N$_4$O$_2$)·2(C$_3$H$_8$O)·54(H$_2$O), M_r = 6795.3, colourless prisms, monoclinic, space group $C2/c$, a = 34.1908(18), b = 41.4283(12), c = 46.9910(18) Å, β = 95.325(5),° V = 66 274(5) Å^3, Z = 8, ρ_{calc} = 1.36 g·cm^{-3}, μ(CuKα) = 1.82 mm^{-1}, θ_{max} = 58.9°, 129 320 reflections measured, 47 500 unique, 4049

parameters, $R = 0.119$, $wR = 0.280$ ($R = 0.289$, $wR = 0.415$ for all data). GooF = 0.92. CCDC 2482201.

Conflicts of interest

There are no conflicts to declare.

Data availability

CCDC 2469726–2469730 (**I–V**), 2482200 and 2482201 (**IV_squeeze** and **V_squeeze**) contain the supplementary crystallographic data for this paper.[56a–g]

The data supporting this article have been included as part of the supplementary information (SI). Supplementary information is available. See DOI: https://doi.org/10.1039/d5ce00666j.

Acknowledgements

Notes and references

1 D.-S. Guo and Y. Liu, *Acc. Chem. Res.*, 2014, **47**, 1925.
2 A.-N. Lazar, F. Perret, M. Perez-Lloret, M. Michaud and A. W. Coleman, *Eur. J. Med. Chem.*, 2024, **264**, 115994.
3 S. Shinkai, K. Araki, T. Matsuda, N. Nishiyama, I. Ikeda, I. Takasu and M. Iwamoto, *J. Am. Chem. Soc.*, 1990, **112**, 9053.
4 J. L. Atwood, L. J. Barbour, M. J. Hardie and C. L. Raston, *Coord. Chem. Rev.*, 2001, **222**, 3.
5 O. Danylyuk and K. Suwinska, *Chem. Commun.*, 2009, 5799.
6 K. Fucke, K. M. Anderson, M. H. Filby, M. Henry, J. Wright, S. A. Mason, M. J. Gutmann, L. J. Barbour, C. Oliver, A. W. Coleman, J. L. Atwood, J. A. K. Howard and J. W. Steed, *Chem. – Eur. J.*, 2011, **17**, 10259.
7 P. C. Leverd, P. Berthault, M. Lance and M. Nierlich, *Eur. J. Org. Chem.*, 2000, **1**, 133.
8 L. J. Barbour and J. L. Atwood, *Chem. Commun.*, 2001, 2020.
9 J. W. Steed, C. P. Johnson, C. L. Barnes, R. K. Juneja, J. L. Atwood, S. Reilly, R. L. Hollis, P. H. Smith and D. L. Clark, *J. Am. Chem. Soc.*, 1995, **117**, 11426.
10 S. J. Dalgarno, M. J. Hardie and C. L. Raston, *Chem. Commun.*, 2004, 2802.
11 I. Ling, Y. Alias, B. W. Skelton and C. L. Raston, *Cryst. Growth Des.*, 2012, **12**, 1564.
12 S. J. Dalgarno, M. J. Hardie, J. L. Atwood and C. L. Raston, *Inorg. Chem.*, 2004, **43**, 6351.
13 M. Makha, C. L. Raston, A. N. Sobolev and A. H. White, *Chem. Commun.*, 2005, 1962.
14 L. Erra, C. Tedesco, G. Vaughan, M. Brunelli, F. Troisi, C. Gaeta and P. Neri, *CrystEngComm*, 2010, **12**, 3463.
15 S. J. Dalgarno, M. J. Hardie, J. L. Atwood, J. E. Warren and C. L. Raston, *New J. Chem.*, 2005, **29**, 649.
16 B. Lesniewska, F. Perret, K. Suwinska and A. W. Coleman, *CrystEngComm*, 2014, **16**, 4399.
17 M. L. Rennie, G. C. Fox, J. Pérez and P. B. Crowley, *Angew. Chem., Int. Ed.*, 2018, **57**, 13764.
18 S. Engilberge, M. L. Rennie, E. Dumont and P. B. Crowley, *ACS Nano*, 2019, **13**, 10343.
19 R. J. Flood, L. Cerofolini, M. Fragai and P. B. Crowley, *Biomacromolecules*, 2024, **25**, 1303.
20 A. Specht, P. Bernard, M. Goeldner and L. Peng, *Angew. Chem., Int. Ed.*, 2002, **41**, 4706.
21 S. J. Dalgarno, J. L. Atwood and C. L. Raston, *Chem. Commun.*, 2006, 4567.
22 I. Ling and C. L. Raston, *Coord. Chem. Rev.*, 2018, **375**, 80.
23 P. B. Crowley, *Acc. Chem. Res.*, 2022, **55**, 2019.
24 N. Lavande, A. Acuña, N. Basílio, V. Francisco, D. D. Malkhedeb and L. Garcia-Rio, *Phys. Chem. Chem. Phys.*, 2017, **19**, 13640.
25 K. Kravets, M. Kravets, V. Sashuk, F. Perret, W. Maskani, D. Albertini, A.-N. Lazar, M. M. Zimnicka and O. Danylyuk, *Chem. – Eur. J.*, 2025, **31**, e202404625.
26 H. Butkiewicz, S. Kosiorek, V. Sashuk, M. Zimnicka and O. Danylyuk, *Cryst. Growth Des.*, 2022, **22**, 2854.
27 Y. Liu, Q. Li, D.-S. Guo and K. Chen, *CrystEngComm*, 2008, **10**, 675.
28 B. Leśniewska, A. W. Coleman, F. Perret and K. Suwińska, *Cryst. Growth Des.*, 2019, **19**, 1695.
29 Y. Liu, W. Liao, Y. Bi, X. Wang and H. Zhang, *Cryst. Growth Des.*, 2009, **9**, 5311.
30 L.-F. Tian, M. Liu, L.-X. Chen, C. Huang, Q.-J. Zhu, K. Chen, J.-L. Zhao and Z. Tao, *Chin. Chem. Lett.*, 2022, **33**, 1524.
31 S. J. Dalgarno, M. J. Hardie, M. Makha and C. L. Raston, *Chem. – Eur. J.*, 2003, **9**, 2834.
32 Y. Liu, Y. Bi, W. He, X. Wang, W. Liao and H. Zhang, *J. Mol. Struct.*, 2009, **919**, 235.
33 J. L. Atwood, S. J. Dalgarno, M. J. Hardie and C. L. Raston, *Chem. Commun.*, 2005, 337.
34 A. N. Lazar, O. Danylyuk, K. Suwinska, R. Kassab and A. W. Coleman, *New J. Chem.*, 2008, **32**, 2116.
35 K. Kravets, M. Kravets and O. Danylyuk, *Cryst. Growth Des.*, 2024, **24**, 10338.
36 A. L. Spek, *Acta Crystallogr., Sect. C:Struct. Chem.*, 2015, **71**, 9.
37 K. Kravets, M. Kravets, K. Kędra and O. Danylyuk, *Supramol. Chem.*, 2021, **33**, 666.
38 F. Perret, V. Bonnard, O. Danylyuk, K. Suwinska and A. W. Coleman, *New J. Chem.*, 2006, **30**, 987.
39 Y. Liu, W. Liao, Y. Bi, M. Wang, Z. Wu, X. Wang, Z. Su and H. Zhang, *CrystEngComm*, 2009, **11**, 1803.
40 O. Danylyuk, H. Butkiewicz, A. W. Coleman and K. Suwinska, *J. Mol. Struct.*, 2017, **1150**, 28.
41 J. M. Alex, P. McArdle and P. B. Crowley, *CrystEngComm*, 2020, **22**, 14.
42 M. Makha, A. N. Sobolev and C. L. Raston, *Chem. Commun.*, 2006, 511.
43 A. Chakraborty, L. R. B. Wilson, S. J. Dalgarno and E. K. Brechin, *Chem. Commun.*, 2025, **61**, 1104.
44 A. Kieliszek and M. Malinska, *Cryst. Growth Des.*, 2021, **21**, 6862.
45 H. Butkiewicz, S. Kosiorek, V. Sashuk, M. M. Zimnicka and O. Danylyuk, *Cryst. Growth Des.*, 2023, **23**, 11.

46 P. R. Lowe, C. E. Sansom, C. H. Schwalbe and M. F. G. Stevens, *J. Chem. Soc., Chem. Commun.*, 1989, 1164.

47 T. Srikrishnan, N. C. De, A. S. Alam and J. Kapoor, *J. Chem. Crystallogr.*, 2004, **34**, 813.

48 R. J. Flood, N. M. Mockler, A. Thureau, M. Malinska and P. B. Crowley, *Cryst. Growth Des.*, 2024, **24**, 2149.

49 K. O. Ramberg, S. Engilberge, T. Skorek and P. B. Crowley, *J. Am. Chem. Soc.*, 2021, **143**, 1896.

50 N. M. Mockler, K. O. Ramberg, F. Guagnini, C. L. Raston and P. B. Crowley, *Cryst. Growth Des.*, 2021, **21**, 1424.

51 J. M. Stokes, C. R. Macnair, B. Ilyas, S. French, J.-P. Côté, C. Bouwman, M. A. Farha, A. O. Sieron, C. Whitfield, B. K. Coombes and E. D. Brown, *Nat. Microbiol.*, 2017, **2**, 17028.

52 N. M. Mockler and P. B. Crowley, *Biophys. Rev.*, 2025, DOI: 10.1007/s12551-025-01323-9.

53 G. M. Sheldrick, *Acta Crystallogr., Sect. C:Struct. Chem.*, 2015, **71**, 3.

54 L. J. Farrugia, *J. Appl. Crystallogr.*, 1999, **32**, 837.

55 E. F. Pettersen, T. D. Goddard, C. C. Huang, G. S. Couch, D. M. Greenblatt, E. C. Meng and T. E. Ferrin, *J. Comput. Chem.*, 2004, **25**, 1605.

56 (a) K. Kravets, M. Kravets and O. Danylyuk, CCDC 2469726: Experimental Crystal Structure Determination, 2025, DOI: 10.5517/ccdc.csd.cc2nwyl3; (b) K. Kravets, M. Kravets and O. Danylyuk, CCDC 2469727: Experimental Crystal Structure Determination, 2025, DOI: 10.5517/ccdc.csd.cc2nwym4; (c) K. Kravets, M. Kravets and O. Danylyuk, CCDC 2469728: Experimental Crystal Structure Determination, 2025, DOI: 10.5517/ccdc.csd.cc2nwyn5; (d) K. Kravets, M. Kravets and O. Danylyuk, CCDC 2469729: Experimental Crystal Structure Determination, 2025, DOI: 10.5517/ccdc.csd.cc2nwyp6; (e) K. Kravets, M. Kravets and O. Danylyuk, CCDC 2469730: Experimental Crystal Structure Determination, 2025, DOI: 10.5517/ccdc.csd.cc2nwyq7; (f) K. Kravets, M. Kravets and O. Danylyuk, CCDC 2482200: Experimental Crystal Structure Determination, 2025, DOI: 10.5517/ccdc.csd.cc2p9xzx; (g) K. Kravets, M. Kravets and O. Danylyuk, CCDC 2482201: Experimental Crystal Structure Determination, 2025, DOI: 10.5517/ccdc.csd.cc2p9y0z.